



# Reservoir sediment characterisation by diffuse reflectance spectroscopy in a semiarid region to support sediment reuse for soil fertilization

Thayslan Carvalho<sup>1</sup> · Arlena Brosinsky<sup>2</sup> · Saskia Foerster<sup>3</sup> · Adunias Teixeira<sup>1</sup> · Pedro Medeiros<sup>4</sup>

Received: 15 February 2022 / Accepted: 13 July 2022 / Published online: 3 August 2022  
© The Author(s) 2022

## Abstract

**Purpose** Soil erosion by water yields sediment to surface reservoirs, reducing their storage capacities, changing their geometry, and degrading water quality. Sediment reuse, i.e., fertilization of agricultural soils with the nutrient-enriched sediment from reservoirs, has been proposed as a recovery strategy. However, the sediment needs to meet certain criteria. In this study, we characterize sediments from the densely dammed semiarid Northeast Brazil by VNIR-SWIR spectroscopy and assess the effect of spectral resolution and spatial scale on the accuracy of N, P, K, C, electrical conductivity, and clay prediction models.

**Methods** Sediment was collected in 10 empty reservoirs, and physical and chemical laboratory analyses as well as spectral measurements were performed. The spectra, initially measured at 1 nm spectral resolution, were resampled to 5 and 10 nm, and samples were analysed for both high and low spectral resolution at three spatial scales, namely (1) reservoir, (2) catchment, and (3) regional scale.

**Results** Partial least square regressions performed from good to very good in the prediction of clay and electrical conductivity from reservoir (< 40 km<sup>2</sup>) to regional (82,500 km<sup>2</sup>) scales. Models for C and N performed satisfactorily at the reservoir scale, but degraded to unsatisfactory at the other scales. Models for P and K were more unstable and performed from unsatisfactorily to satisfactorily at all scales. Coarsening spectral resolution by up to 10 nm only slightly degrades the models' performance, indicating the potential of characterizing sediment from spectral data captured at lower resolutions, such as by hyperspectral satellite sensors.

**Conclusion** By reducing the costly and time-consuming laboratory analyses, the method helps to promote the sediment reuse as a practice of soil and water conservation.

**Keywords** Sediment characterization · Spectroscopy · Sediment reuse · Surface reservoirs · Semiarid · Brazil

Responsible editor: Simon Pulley

✉ Saskia Foerster  
foerster@gfz-potsdam.de

<sup>1</sup> Department of Agricultural Engineering, Federal University of Ceará – UFC, Av. Humberto Monte - Campus do Pici, Bloco 804, Fortaleza 60455-760, Ceará, Brazil

<sup>2</sup> Institute of Environmental Science and Geography, University of Potsdam, Karl-Liebknecht-Str. 24-25, 14476 Potsdam, Germany

<sup>3</sup> Section 1.4 Remote Sensing and Geoinformatics, Helmholtz Centre Potsdam GFZ German Research Centre for Geosciences, Telegrafenberg, Potsdam 14473, Germany

<sup>4</sup> Federal Institute of Education, Science and Technology of Ceará - IFCE, Av. Parque Central, 1315, Maracanaú 61939-140, Ceará, Brazil

## 1 Introduction

Soil is an essential component of the Earth's system, linked directly with the hydrological cycle, sedimentological, geochemical, biological, and ecological processes, as well as representing a major source of goods, services, and resources for humanity (Brevik et al. 2015; Decock et al. 2015). However, the current production model to meet the increasing demand for food, fibre, and fuel from the world's growing population has accelerated land degradation (Tesfaye et al. 2015; Ollobarren et al. 2016).

The pursuit for increasing crop productivity and the expansion of new areas for cultivation increase the pressure on fragile lands and ecosystems, impacting hydrological processes and favouring water erosion (Wohl et al. 2012; Santos et al. 2016). Soil erosion by water may occur at different

intensities depending on the characteristics of rainfall, as well as terrain, soil type, and land cover and use. Soils in the Brazilian semiarid region are usually shallow with low organic matter content and low water retention capacity. These characteristics, in association with the high intensity rainfall events typical of this region, and the absence of vegetation cover resulting from inadequate land use, can potentialize the erosive process (Calixto Júnior and Drumond 2014).

The material produced by erosion is exported to the river systems, and a significant portion may be deposited in reservoirs used for water supply. In the semiarid region of Brazil, sediment deposition causes a reduction of approximately 1.6% of the storage capacity of surface reservoirs per decade (de Araújo et al. 2006). Thereby, sediment deposition also changes reservoir geometry, making them shallower and more susceptible to evaporation (de Araújo et al. 2006). Besides, soil erosion contributes to reservoir eutrophication, since the nutrient-enriched sediments increase ecosystem productivity and reduce the dissolved oxygen level (Coelho et al. 2017; Moura et al. 2020).

In theory, soil conservation practices are effective in reducing sediment yield and reservoir siltation; however, human and financial resources needed for land use control and monitoring may hamper implementation to large territorial extensions. From the reservoir perspective, removal and reuse of the deposited sediment have potential to, simultaneously, reduce the nutrient content in the lake and replace its storage capacity lost by siltation (Lira et al. 2020). Sediment reuse has been proposed as a practice contributing to the circular economy concept, considering sediment as a resource rather than waste (Brils et al. 2014), and many studies emphasize its positive effects (e.g., Fonseca et al. 1998; Sigua 2009; Junakova and Balintova 2012; Mattei et al. 2017; Braga et al. 2019). Capra et al. (2015) reported on the reuse of dredged sediment for the replacement of soil degraded by erosion, concluding that the addition of sediment had beneficial effects on the physicochemical properties of the soil and resulted in higher total dry matter production in plants. Also, Sigua et al. (2004) observed increases in biomass production when they reused dredged sediment, and Braga et al. (2017) found that the addition of sediment in sunflower cultivation improved the relative chlorophyll content and total dry mass when compared to plants growing on substrate containing commercial fertilizers.

Although the economic feasibility of sediment reuse for soil fertilization has already been demonstrated for specific conditions (e.g., Braga et al. 2019), the agricultural sector has not yet adopted this practice to replace traditional fertilization, which, via soil erosion, may further increase reservoir eutrophication. Therefore, sediment characterization is essential to provide information about its suitability as fertilizer and to promote the idea of reuse, consolidating this

practice in the agricultural production system as a measure of soil and water conservation, as well as financial benefit.

Such sediment characterization can be achieved by several means, such as time-consuming and costly physicochemical laboratory analyses. Currently, visible near-infrared and short-wave infrared (VNIR-SWIR) spectroscopy has proven to be an alternative for indirect analyses of soil or sediment attributes, as it (i) is cheaper and faster than the traditional laboratory procedures and thus (ii) favours repeatability and reproducibility at different temporal and spatial scales. Recent research has successfully established correlations between VNIR-SWIR spectroscopy and sediment or soil attributes, for instance Viscarra Rossel et al. (2006a), Vågen et al. (2006), Morgan et al. (2009), Kuang and Mouazen (2011), Nawar et al. (2017), Morellos et al. (2016), Cozzolino et al. (2016), Hu (2013), Wang et al. (2015), and Demattê et al. (2019a).

Thereby, sediment characterization is especially viable in semiarid regions due to the flood-drought dynamics: In Northeast Brazil, where this study was conducted, small and medium-sized reservoirs often fall dry during the intra-annual dry season, exposing the silted sediment and making it easily accessible. This increases the chance that the sediment can be periodically sampled and analysed, e.g., by VNIR-SWIR spectroscopy and, consequently, be easily excavated and reused when proven efficient for soil fertilization.

To assess the potential of VNIR-SWIR spectroscopy for the characterization of reservoir sediments, we collected sediment samples, performed physicochemical and spectral analyses, and generated regression models with the goals to (i) characterize the sediment deposited in reservoirs in the semiarid Northeast of Brazil; thereby, we also aimed to (ii) assess the effect of spatial scale on the accuracy of prediction models; in addition, to assess the potential of spaceborne imaging spectroscopy data that is currently becoming more available, we (iii) assessed the influence of spectral resolution on model performance.

## 2 Study area

This study was conducted in the semiarid region of Brazil, Federal State of Ceará, encompassing ten surface reservoirs of various sizes (flooded areas varying from 0.02 to 37 km<sup>2</sup>) distributed in three catchments (Benguê, Fogareiro, and Pentecoste, with approximately 1000, 5100, and 3200 km<sup>2</sup>, respectively), as illustrated in Fig. 1.

Climate in the region is semiarid, with annual potential evaporation ranging from approximately 1800 mm by the coast to up to 3000 mm in the upstream hinterland. Average annual precipitation presents an inverse gradient pattern, ranging from roughly 1100 to 550 mm, concentrated in a

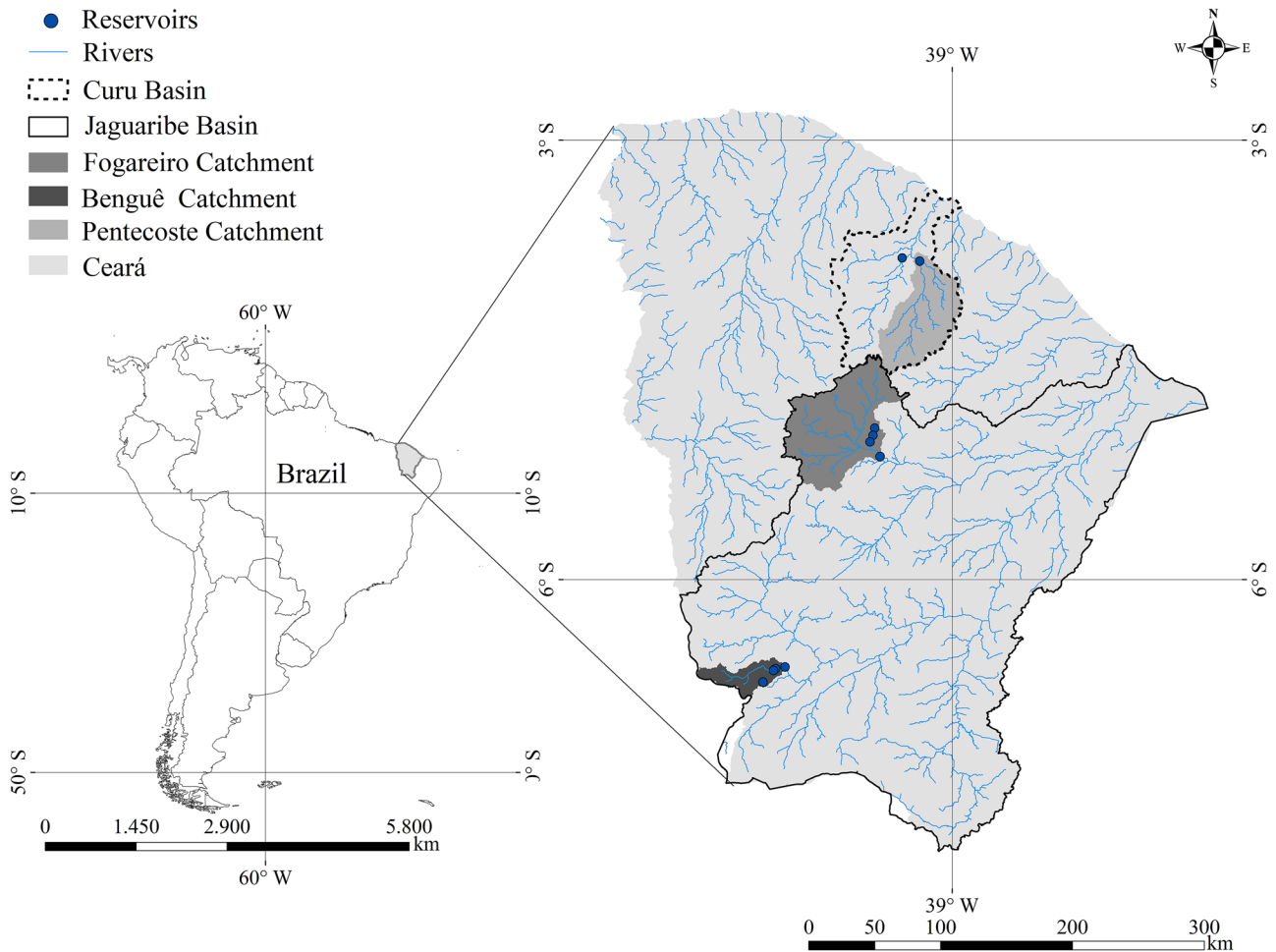


**Fig. 1** Study area in the semiarid northeast of Brazil

well-defined rainy season, which generates 6 to 9 months per year of atmospheric water deficit, on average (INMET 2018).

Additionally, shallow soils (usually < 1 m depth) on top of a crystalline basement make the rivers intermittent and promote low hydrogeological potential in the region, which led to the construction of dams for water supply. The reservoir network, with an average density of the order of one reservoir per 8 km<sup>2</sup>, impacts the overall water resources (de Araújo and Medeiros 2013), and is particularly important on sediment retention (Medeiros et al. 2014; Mamede et al. 2018). The accumulation of sediment and the adsorbed nutrients in the reservoirs results in a *water quality effect*, as described by Medeiros and Sivapalan (2020), negatively affecting water availability in terms of quantity (reservoir siltation) and quality (eutrophication). In this context, sediment reuse has been proposed for soil fertilization (Braga et al. 2019), also contributing to recovery of water quality (Lira et al. 2020).

The wide range of reservoirs and catchment areas assessed in this study enabled an analysis of the potential of sediment characterization by VNIR-SWIR spectroscopy at the reservoir (< 40 km<sup>2</sup>), catchment (900–6000 km<sup>2</sup>) and regional (82,500 km<sup>2</sup>) spatial scales. Analysis at the reservoirs Araras, Açude III, Boqueirão, Benguê, and Escola was not possible due to the limited number of sediment samples in each of those reservoirs, but such samples were included in the analysis at the catchment and regional scales. Table 1 presents the reservoirs and catchments adopted in each of the spatial scales, and a description of each area is presented below.

The studied reservoirs and catchments were selected based on the following criteria:

- Variability in terms of soil type and hydrological regime, which control the sediment characteristics and flux;

**Table 1** Reservoirs and catchments assessed in this study

Regional scale	Catchment scale	Reservoir scale	Reservoir area (km <sup>2</sup> )	Reservoir <i>n</i> <sup>a</sup>
Jaguaribe and Curu basins (82,500 km <sup>2</sup> ) <i>n</i> <sup>a</sup> = 138	Benguê (964 km <sup>2</sup> ) <i>n</i> <sup>a</sup> = 28	Araras <sup>b</sup>	0.02	5
		Açude III <sup>b</sup>	0.02	5
		Boqueirão <sup>b</sup>	0.03	12
		Benguê <sup>b</sup>	2.23	6
	Fogareiro (5106 km <sup>2</sup> ) <i>n</i> <sup>a</sup> = 80	São Nicolau	0.42	20
		São Joaquim	1.20	20
		Marengo	3.39	20
		Fogareiro	20.46	20
	Pentecoste (3238 km <sup>2</sup> ) <i>n</i> <sup>a</sup> = 30	Escola <sup>b</sup>	0.03	10
		Pentecoste	36.88	20

<sup>a</sup>Number of sediment sampling points

<sup>b</sup>Reservoirs not analysed individually due to limited number of samples

- Existence of strategic reservoirs at the catchments' outlets, monitored by the Water Resources Management Company of Ceará — COGERH, which provides secondary data on hydrological variability;
- Scientific research conducted by the authors in the regions during the last decades, which contributes to prior knowledge.

## 2.1 Benguê catchment

The Benguê catchment drains an area of roughly 1000 km<sup>2</sup> in the headwaters of the Jaguaribe Basin, with 560 mm average annual rainfall producing 47 mm of runoff (8% runoff coefficient) (Ceará 2009). Predominant soil types are luvisols and neosols, though deep latosols prevail in the border regions (EMBRAPA 2011). The catchment is controlled by the Benguê reservoir at its outlet, with a storage capacity of 19.6 hm<sup>3</sup> and a flooded area of 3.5 km<sup>2</sup>. In addition to the Benguê reservoir, three small reservoirs with flooded areas ranging from 0.02 to 0.03 km<sup>2</sup> were studied: Boqueirão (de Figueiredo et al. 2016), Araras, and Açude III. Figure 1 of the supplementary material (Fig. S1) presents the location of the studied reservoirs and the respective sediment sampling points in the Benguê catchment.

## 2.2 Fogareiro catchment

Alike Benguê, the Fogareiro catchment is located in the Jaguaribe Basin, with an area of approximately 5100 km<sup>2</sup> with predominance of neosols, but also luvisols and argisols (EMBRAPA 2011). Average annual rainfall is 680 mm and runoff 58 mm, which corresponds to 8% runoff coefficient. Four reservoirs were studied in the catchment: Fogareiro, Marengo, São Joaquim, and São Nicolau, with storage capacities of 118, 15.3, 5.0, and 0.9 hm<sup>3</sup>, and flooded areas

of 20.5, 3.4, 1.2, and 0.4 km<sup>2</sup>, respectively. Studies have been conducted in the Fogareiro catchment for characterization of surface reservoirs (Zhang et al. 2016, 2018) as well as the feasibility of the sediment reuse practice (Braga et al. 2019). Fig. S2 (supplementary material) presents the location of the studied reservoirs and the respective sediment sampling points in the Fogareiro catchment.

## 2.3 Pentecoste catchment

The Pentecoste catchment is located within the Curu Basin and extends over an area of approximately 3200 km<sup>2</sup>. Average annual rainfall and runoff account for 750 and 126 mm, respectively, corresponding to a runoff coefficient of 17% (Ceará 2009). Most of the area is on luvisols, though also small areas of planosols are indicated (EMBRAPA 2011). In this catchment, two reservoirs were selected for sediment sampling: the Pentecoste reservoir, located at the catchment outlet, with 360 hm<sup>3</sup> storage capacity and a flooded area of 57 km<sup>2</sup>, and the Escola reservoir, located in the Vale do Curu Experimental Farm (FEVC), with a storage capacity of approximately 0.05 hm<sup>3</sup> and a flooded area of 0.03 km<sup>2</sup>, monitored since 2015 (Silveira and Mamede 2021) (Fig. S3, supplementary material).

## 3 Material and methods

The study comprehends four steps: (1) sediment sampling in the studied reservoirs; (2) physicochemical laboratory analyses; (3) spectral analyses; (4) correlation of physicochemical and spectral properties to elaborate models of reservoir sediment characterization by diffuse reflectance spectroscopy at different spectral and spatial resolutions.

### 3.1 Sediment sampling

Sediment sampling was performed in empty reservoirs in the period of November 2016 to February 2017. Small reservoirs dry out periodically in the study region due to the high evaporation rates, whereas medium and large size reservoirs retain water for longer periods. However, due to a long-lasting drought (2012 to 2017), it was possible to obtain sediment samples also from larger strategic reservoirs. The sediment sampling from the reservoirs' beds was preceded by removal of litter (Fig. 2). At each sampling point, an area of roughly 0.5 m diameter was delimited and approximately 2 kg of sediment from the top layer (~2 cm depth) was collected at 3 to 5 points, forming a composite sample. The number of composite samples varied according to the size of the reservoir, with twenty samples being the maximum for the largest reservoirs (see Table 1), totalling 138 in the 10 studied reservoirs.

The sediment samples were air-dried, disaggregated, homogenized, and sieved to 2 mm, and then sent to physicochemical and spectral laboratories for the respective analyses, as described below.

### 3.2 Physicochemical analyses of sediment

The sediment physicochemical analyses were performed in the Soil and Water Laboratory of the Federal University of Ceará (UFC). The attributes nitrogen (N), phosphorus (P), potassium (K), soil organic carbon (SOC), and electrical conductivity (EC) and granulometry (for clay content) were analysed according to the methods recommended in the Manual of Soil Analysis Methods of the Brazilian Agricultural Research Corporation (EMBRAPA 2017):

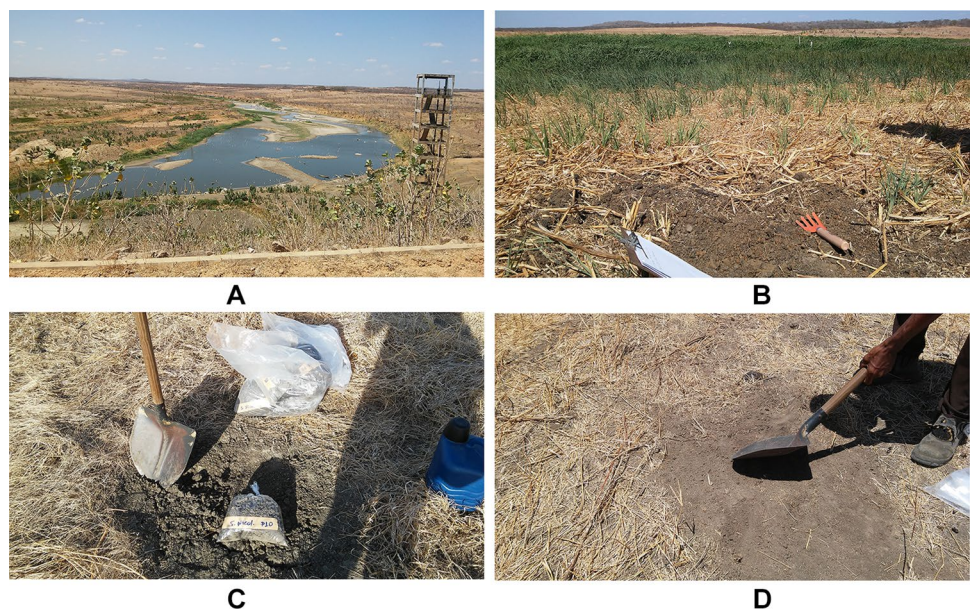
- N ( $\text{g kg}^{-1}$ ): Kjeldahl method, in which N is converted to ammonium sulphate through oxidation, and the released ammonia is determined by acidimetry;
- P ( $\text{mg kg}^{-1}$ ): formation of blue phosphorus-molybdc complex after reduction of molybdate with ascorbic acid, and determination of the assimilable phosphorus by molecular absorption spectrophotometry;
- K ( $\text{cmol}_c \text{ kg}^{-1}$ ): extraction with dilute hydrochloric acid solution and subsequent determination of the exchangeable potassium by flame spectrophotometry;
- SOC ( $\text{g kg}^{-1}$ ): oxidation of organic matter via a wet process with potassium dichromate in a sulfuric medium. The excess dichromate after oxidation is titrated with a standard solution of ferrous ammonium sulphate;
- EC ( $\text{dS m}^{-1}$ ): preparation of a saturation paste by addition of water to the sediment sample until saturation, and direct reading with a conductivity meter;
- Clay fraction ( $\text{g kg}^{-1}$ ): pipette method, with agitation and suspension of the silt and clay fractions in dispersing solution, and quantification of the suspended fraction after sedimentation.

During control procedures and uncertainty assessments, the laboratory performs triplicate analyses and usually observes <2% differences, with a 5% difference being admitted as the upper limit for reanalyses. Although no triplicate analyses were performed in this study, we assume the laboratory error to be <5%.

### 3.3 Spectral analyses of sediment

For the spectral analyses, sediment samples were air-dried and placed in black cylindrical plastic containers with 6 cm

**Fig. 2** Study area and field work: **A** Fogareiro reservoir with low water level, **B** bed of an empty reservoir **C** litter removal at a sampling point, **D** sediment sampling



diameter and 4 cm depth, totalling a volume of 113.1 cm<sup>3</sup>. The readings were taken at the Agricultural and Electronics Laboratory (LEMA) of UFC in a dark room with no reflective surfaces. A spectroradiometer covering the spectral range between 350 and 2500 nm (ASD FieldSpec<sup>®</sup>3 Hi-Res) was used with a single artificial light source (halogen lamp) oriented to the sample with a 45° zenith angle and 71 cm distance. The distance between sensor head and sample was one-third of the container diameter, to avoid influence of the edges on the readings. Each spectrum was obtained by automatic averaging of 30 measurements, and three spectra were collected from each sample with 120° rotation between readings. During the analysis, three optimizations and white reference measures were performed, the first prior to the spectral readings and the last two when the equipment indicated saturation.

The spectral reading comprises the range between 350 and 2,500 nm with 1 nm spectral resolution. However, due to noise observed in the border areas of the measured spectral range, only the region between 400 and 2400 nm was considered for subsequent analyses.

### 3.4 Models of sediment characterization from spectroscopy

Establishing relationships between soil/sediment physicochemical properties and reflectance data is challenging due to the large number of possible combinations. Currently, partial least squares regression — PLSR (see Wold et al. 2001) is a widely used and successful technique for estimating target characteristics from spectral data (e.g., Viscarra Rossel et al. 2006a, 2008; Gomez et al. 2008; Lu et al. 2013; Ludwig et al. 2017). The PLSR algorithm selects orthogonal factors that maximize the covariance between the predictor variables  $X$  (spectral data) and the response variable  $Y$  (sediment attribute, in this case) and decomposes both  $X$  and  $Y$  variables to find new components (scores), called latent variables, which are orthogonal. Regressions are calculated between these new components of variables  $X$  and  $Y$  (Moreira et al. 2015).

In our study, we used the ParLeS version 3.1 software provided by Viscarra Rossel (2008) to estimate the contents of N, P, K, SOC, EC, and clay from spectral data via PLSR-modelling. Prior to PLSR-modelling, pre-processing techniques were applied to improve the robustness of the models. First, detector jumps present in a few occasions were corrected routinely using in-house scripts. Then, ParLeS “spectral manipulation” options were applied, namely, (1) a SNV transformation (Barnes et al. 1989) for spectral normalization to remove interference due to light scattering,

(2) a Savitzky-Golay filter (Savitzky and Golay 1964) for spectral smoothing, and (3) mean centring of the data. In our case, this selection was found to outperform other common pre-processing techniques such as e.g., spectral derivatives.

The regression models were developed individually for each of the reservoirs and catchments presented in Table 1, except those with less than 20 sediment samples, resulting in five reservoir models, three catchment models, and one basin model per sediment property (totalling 54 calibrated models). Due to the low number of samples in individual reservoirs ( $n < 20$ ) and for reasons of comparability between model performances, we did not separate the datasets into calibration and validation, but performed leave-one-out cross validation, whereas a maximum number of 12 factors were allowed. Further, we provide regression coefficients (intercept and slope) and bias of the calibrated models. Mean, standard deviation and range of observed versus predicted sediment attributes are presented in the supplementary material.

Performance of the regression models was assessed as the best combination of high coefficient of determination ( $R^2$ ) and low root-mean-square error (RMSE), while aiming for a ratio of performance to deviation (RPD)  $> 1.4$ . Usual ranges of RPD are taken as excellent (RPD  $> 2.50$ ), very good ( $2.00 < \text{RPD} \leq 2.50$ ), good ( $1.80 < \text{RPD} \leq 2.00$ ), moderate ( $1.40 < \text{RPD} \leq 1.80$ ), weak ( $1.00 < \text{RPD} \leq 1.40$ ), and very poor ( $\text{RPD} \leq 1.00$ ) (Viscarra Rossel et al. 2006b). In addition, Nash–Sutcliffe efficiency (NSE) coefficient was calculated as measure of model performance, according to which the model can be considered very good ( $0.75 < \text{NSE} \leq 1.00$ ), good ( $0.65 < \text{NSE} \leq 0.75$ ), satisfactory ( $0.50 < \text{NSE} \leq 0.65$ ), or unsatisfactory ( $\text{NSE} \leq 0.50$ ) (Moriassi et al. 2007).

To analyse the influence of spectral resolution on the accuracy of sediment attribute estimation from spectroscopic data, the original spectral curves of 1 nm resolution (2001 spectral bands) as provided by the instrument were resampled to 5, and 10 nm resolution, resulting in 400, and 200 bands, respectively. For each of the abovementioned spectral resolutions, the model presenting highest correlation with each sediment attribute, estimated from the physicochemical analyses, was selected. Again, the respective coefficients of determination ( $R^2$ ) were used as a measure of the goodness of fit.

To assess the influence of spatial scale on the estimations, the physicochemical data of the sediment sampling points were grouped at spatial scales varying from reservoir ( $< 100 \text{ km}^2$ ) to regional ( $> 10,000 \text{ km}^2$ ), according to Table 1.  $R^2$  were calculated for all combinations of sediment attributes and spatial scales, enabling to interpret how the correlation evolves.

## 4 Results and discussion

### 4.1 Physicochemical and spectral characterization of the sediments

Sediment properties in the 10 studied reservoirs are summarized in Table 2, from which the variation within and between reservoirs can be observed. The largest variation among the reservoirs was observed in P content, with a minimum of 2 mg kg<sup>-1</sup> in a sample of the Benguê reservoir and a maximum of 289 mg kg<sup>-1</sup> in São Nicolau. Mean P values in those same reservoirs were 7 mg kg<sup>-1</sup> and 82 mg kg<sup>-1</sup>, respectively.

Nitrogen, K, and SOC tend to be less variable among the studied reservoirs, with mean values ranging from 1.3 to 1.9 g kg<sup>-1</sup>, 0.8 to 2.0 cmol<sub>c</sub> kg<sup>-1</sup>, and 13.4 to 19.0 g kg<sup>-1</sup>, respectively. As for P, clay contents showed a large variation, with the highest value observed in the Pentecoste reservoir (maximum of 744 g kg<sup>-1</sup>), where the mean was 528 g kg<sup>-1</sup>, and lowest in the Escola reservoir (minimum and mean of 37 and 249 g kg<sup>-1</sup>, respectively). Mean values of EC ranged from a minimum of 1.5 to a maximum 6.7 dS m<sup>-1</sup> in the Benguê and Escola reservoirs, respectively. Within each reservoir, the standard deviation ranged from 0.6 to 5.6 dS m<sup>-1</sup>.

The spectra of the sediment in all sampling points are shown in Fig. 3 (Benguê catchment), Fig. 4 (Fogareiro catchment), and Fig. 5 (Pentecoste catchment). There is little, visually expressive contrast among the different catchments. Some variability can be observed in the VNIR between 500 and 900 nm (likely linked to Carbon and sediment colour), slope between 1500 and 1800 nm (Carbon, grain size), and the water absorption features around 1400 and 1900 nm; all sediment spectra seem to contain a more or less distinct clay feature around 2200 nm. The overall reflectance (brightness) varies within each reservoir, in a narrow range for the Boqueirão reservoir (Fig. 3) and a wide range, e.g., for the Marengo reservoir (Fig. 4).

### 4.2 Performance of models for sediment characterization from spectroscopy

#### 4.2.1 Reservoir-scale

Performance of the models for characterization of sediments from spectroscopy at the reservoir-scale (< 40 km<sup>2</sup>) using partial least squares regressions is presented in Fig. 6 and Table 3, which show the cross-validation results for N, P, K, SOC, clay, and electrical conductivity. Please consider that the models were established for each of the five reservoirs individually, although results are presented together in Fig. 6A–F for comparison.

In general, regression models to estimate clay, EC, and SOC presented the highest correlations between spectra and sediment properties (with  $R^2$  in the range of 0.49 to 0.85) and best performances, varying from satisfactory to very good according to NSE coefficient (values in the range of 0.48 to 0.84) and from moderate to excellent as interpreted according to RPD (most models falling in the range of  $1.40 < \text{RPD} < 2.00$ , classified as moderate to good). Models for N presented moderate correlations as well ( $R^2$  in the range of 0.52 to 0.69), with performances classified as satisfactory to good according to NSE (in the range of 0.47 to 0.66) and moderate according to RPD (minimum of 1.42 and maximum of 1.75). However, the models for P and K performed unsatisfactorily to satisfactorily according to NSE coefficient ( $0.22 \leq \text{NSE} \leq 0.51$  and  $0.05 \leq \text{NSE} \leq 0.62$ , respectively) and from weak to moderate according to RPD ranges ( $1.16 \leq \text{RPD} \leq 1.47$  and  $1.05 \leq \text{RPD} \leq 1.67$ , respectively). Among the reservoirs, models for Marengo and Fogareiro performed better ( $R^2$  in the ranges of 0.45 to 0.85 and 0.49 to 0.75, respectively; NSE from 0.44 to 0.84 and 0.46 to 0.75, respectively; RPD in the ranges of 1.37 to 2.59 and 1.40 to 2.06, respectively), whereas the results for Pentecoste presented high variation (NSE,  $R^2$ , and RPD varying from 0.05 to 0.83, 0.08 to 0.83 and 1.05 to 2.47, respectively).

#### 4.2.2 Catchment-scale

Results of models for sediment characterization at the catchment-scale (900–6000 km<sup>2</sup>) are presented in Fig. 7, whereas performance of the models is presented in Table 4. Again, please consider that the models were established for each catchment individually, although they are presented altogether in the graphs of Fig. 7A–F for comparison.

Alike the performance at the reservoir scale, regression models to estimate clay and EC usually presented coefficients of determination in the range of 0.4 to 0.8 and performances classified from satisfactory to very good according to NSE coefficient and from moderate to very good according to RPD. However, low correlation was observed between spectra and EC at the Pentecoste catchment ( $R^2 = 0.12$ ), where the model performed unsatisfactorily (with  $\text{NSE} = 0.06$  and  $\text{RPD} = 1.05$ ), strongly influenced by an extreme value equivalent to almost five times the average. It is important to note that removal of such extreme value did not considerably improve the modelling results; therefore, we decided to keep all values.

The SOC, N, P, and K models performed unsatisfactorily based on NSE ( $\text{NSE} < 0.5$ ) and weak based on RPD ( $\text{RPD} < 1.4$ ) in general, with some specific ones presenting satisfactory/moderate results: SOC and N at the Fogareiro catchment and P and K at the Benguê catchment.

**Table 2** Statistics of sediment attributes for the three study catchments

Catchment	Reservoir		N (g kg <sup>-1</sup> )	P (mg kg <sup>-1</sup> )	K (cmol <sub>c</sub> kg <sup>-1</sup> )	SOC (g kg <sup>-1</sup> )	Clay (g kg <sup>-1</sup> )	EC (dS m <sup>-1</sup> )
Benguê catchment	Araras*	Mean	1.6	45.6	1.6	16.1	350	2.4
		SD	0.4	56.8	0.4	4.2	138	1.1
		Min	0.9	14.0	1.0	9.2	112	1.4
		Max	1.9	147.0	2.0	20.3	473	4.1
		Skewness	-1.9	2.2	-1.9	-1.4	-1.8	1.3
	Açude III*	Mean	1.8	16.4	1.6	17.8	337	1.6
		SD	0.9	7.5	0.7	9.3	103	1.6
		Min	0.3	8.0	0.8	2.8	190	0.2
		Max	2.5	28.0	2.3	27.2	447	3.9
		Skewness	-1.6	0.9	-0.4	-1.2	-0.6	1.0
	Benguê*	Mean	1.8	7.3	0.8	17.9	273	1.5
		SD	0.8	6.5	0.4	7.9	161	0.7
		Min	0.4	2.0	0.2	4.4	36	0.4
		Max	2.6	19.0	1.2	24.2	445	2.5
		Skewness	-1.3	1.4	-0.5	-1.3	-0.8	-0.5
Boqueirão*	Mean	1.5	14.9	1.3	15.3	344	1.6	
	SD	0.4	3.6	0.5	3.6	78	0.6	
	Min	1.2	9.0	0.7	11.4	225	0.7	
	Max	2.1	22.0	2.4	22.7	431	2.4	
	Skewness	0.6	0.2	0.7	0.9	-0.4	-0.6	
Fogareiro catchment	Fogareiro	Mean	1.9	22.0	1.2	19.0	474	4.0
		SD	0.5	8.3	0.6	5.0	171	1.9
		Min	0.8	9.0	0.4	7.1	66	0.4
		Max	2.6	52.0	3.6	24.4	665	7.8
		Skewness	-0.8	2.5	2.7	-1.2	-1.3	0.0
	Marengo	Mean	1.3	10.9	1.6	13.4	273	2.8
		SD	0.7	4.8	1.3	6.2	251	4.3
		Min	0.3	4.0	0.3	3.5	10	0.2
		Max	2.5	20.0	4.9	23.4	704	17.2
		Skewness	0.2	0.1	1.1	0.2	0.6	2.4
	São Joaquim	Mean	1.8	26.2	2.0	18.5	368	1.9
		SD	0.7	12.9	0.9	5.9	172	1.2
		Min	0.5	10.0	0.7	5.8	34	0.5
		Max	2.7	62.0	4.3	24.8	668	4.5
		Skewness	-0.8	1.5	0.6	-1.0	-0.3	0.6
São Nicolau	Mean	1.7	81.9	0.9	17.0	269	3.2	
	SD	0.7	68.7	0.6	7.5	124	4.0	
	Min	0.4	17.0	0.2	4.3	130	0.5	
	Max	2.5	289.0	2.9	29.6	563	15.2	
	Skewness	-0.3	2.0	1.9	-0.1	1.1	2.1	
Pentecoste catchment	Escola*	Mean	1.7	15.7	1.7	16.6	249	6.7
		SD	0.9	6.3	0.8	8.4	165	5.6
		Min	0.5	7.0	0.5	5.0	37	0.7
		Max	2.5	27.0	2.9	26.0	541	21.6
		Skewness	-0.6	0.3	-0.3	-0.5	0.3	2.3



**Table 2** (continued)

Catchment	Reservoir		N (g kg <sup>-1</sup> )	P (mg kg <sup>-1</sup> )	K (cmol <sub>c</sub> kg <sup>-1</sup> )	SOC (g kg <sup>-1</sup> )	Clay (g kg <sup>-1</sup> )	EC (dS m <sup>-1</sup> )
	Pentecoste	Mean	1.6	10.3	1.8	15.7	528	4.4
		SD	0.6	4.3	0.8	5.4	221	2.5
		Min	0.2	5.0	0.4	2.6	11	0.4
		Max	2.4	22.0	3.9	23.5	744	8.2
		Skewness	-0.6	1.7	0.6	-0.6	-1.2	-0.2

\*Reservoirs not analysed individually, but only as part of a catchment, due to limited number of samples

Correlations were also lower than those obtained for the previous properties, with  $R^2$  usually below 0.6 and as low as 0.01. It is important to note the very poor performance of SOC and N models at the Benguê catchment, with  $NSE < 0$  and  $RPD \leq 1.0$ . Negative NSE indicates that taking the average values of the samples is a better estimate than adopting the tested model.

#### 4.2.3 Regional-scale

Figure 8 illustrates the results of sediment characterization from spectroscopy at the regional-scale, which comprises the sediment samples from all reservoirs in the Jaguaribe and Curu basins (total area of 82,500 km<sup>2</sup>). Contrary to Figs. 6 and 7, these graphs show only one model each. Models' performance is shown in Table 5.

At the regional scale, the models for clay and EC presented good and moderate to good performance according

to NSE (values of 0.65 and 0.69, respectively) and RPD (values of 1.70 and 1.81, respectively). The coefficients of determination were 0.65 and 0.69, indicating some level of correlation. The models for SOC, N, P, and K presented NSE values ranging from 0.20 to 0.39 (classified as unsatisfactory) and RPD values ranging from 1.12 to 1.29 (classified as weak), at this scale. Lower correlations were obtained between spectra and those properties, with  $0.24 \leq R^2 \leq 0.42$ .

#### 4.2.4 Discussion

In this study, models' performances expressed by NSE and RPD tend to decrease in models with low slope, i.e., when the dependent variable is less sensitive to the variation of the input data. For instance, slopes of the calibrated models at the reservoir scale are mostly in the range of 0.5 to 0.9. Some exceptions are K in the São Nicolau and Pentecoste reservoirs, and also P for the latter, in which the lowest NSE

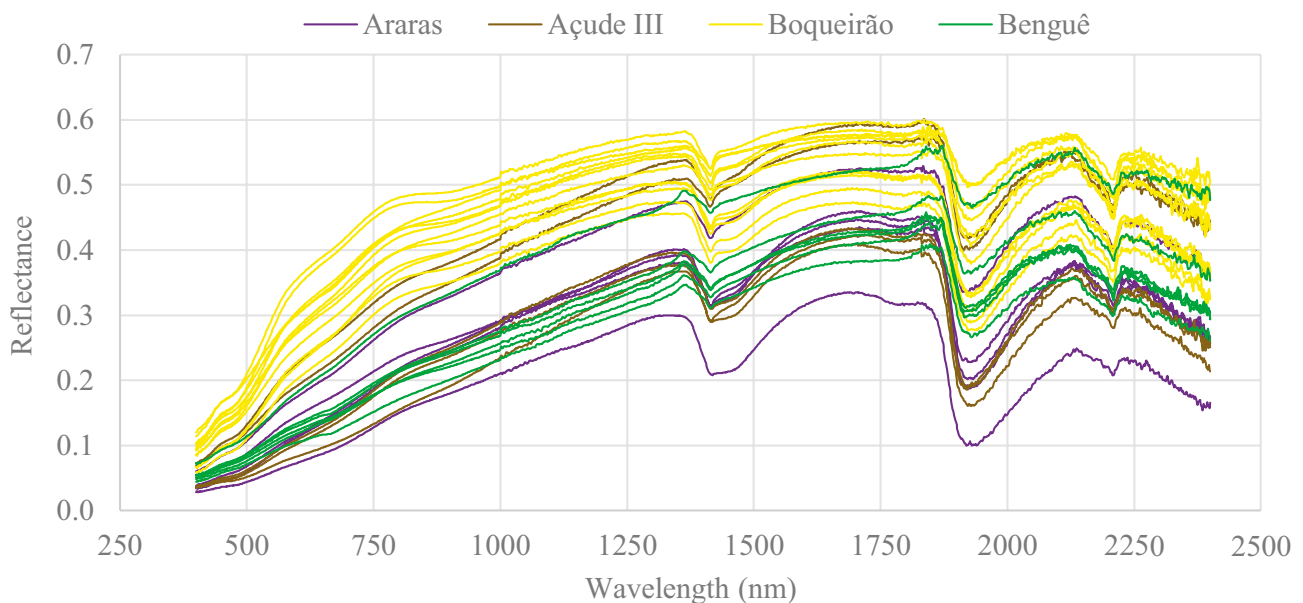


**Fig. 3** Spectra of the sediment samples in the Benguê catchment, before pre-processing

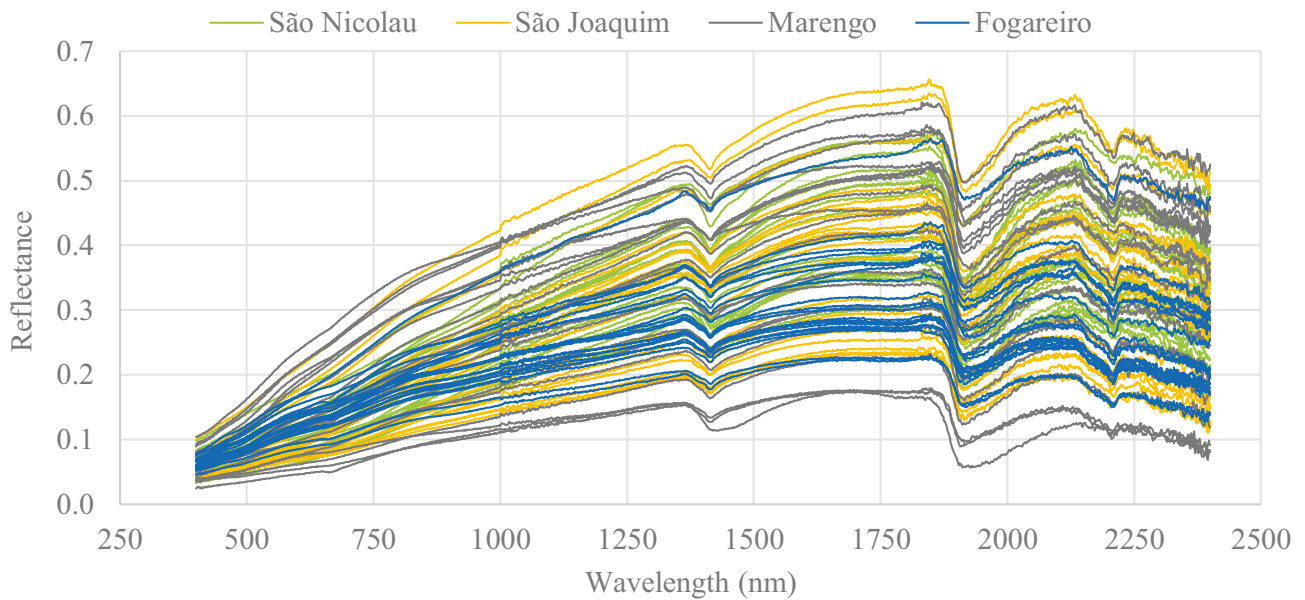


**Fig. 4** Spectra of the sediment samples in the Fogareiro catchment, before pre-processing

(0.23, 0.05, and 0.22, respectively) and RPD (1.17, 1.05, and 1.16, respectively) are observed.

In summary, the models for clay and EC performed in the range of good to very good at the spatial scales ranging from reservoirs (<40 km<sup>2</sup>) up to regional (>82,500 km<sup>2</sup>), with some specific ones rated as satisfactory. SOC models performed satisfactorily to very good at the reservoir scale,

but degraded to unsatisfactory at the other scales. Similar results were found for N, whose models were satisfactory at the reservoir scale but tended to be unsatisfactory at the catchment and regional scales. The models for P and K presented high variation, from unsatisfactory to satisfactory at all investigated scales.

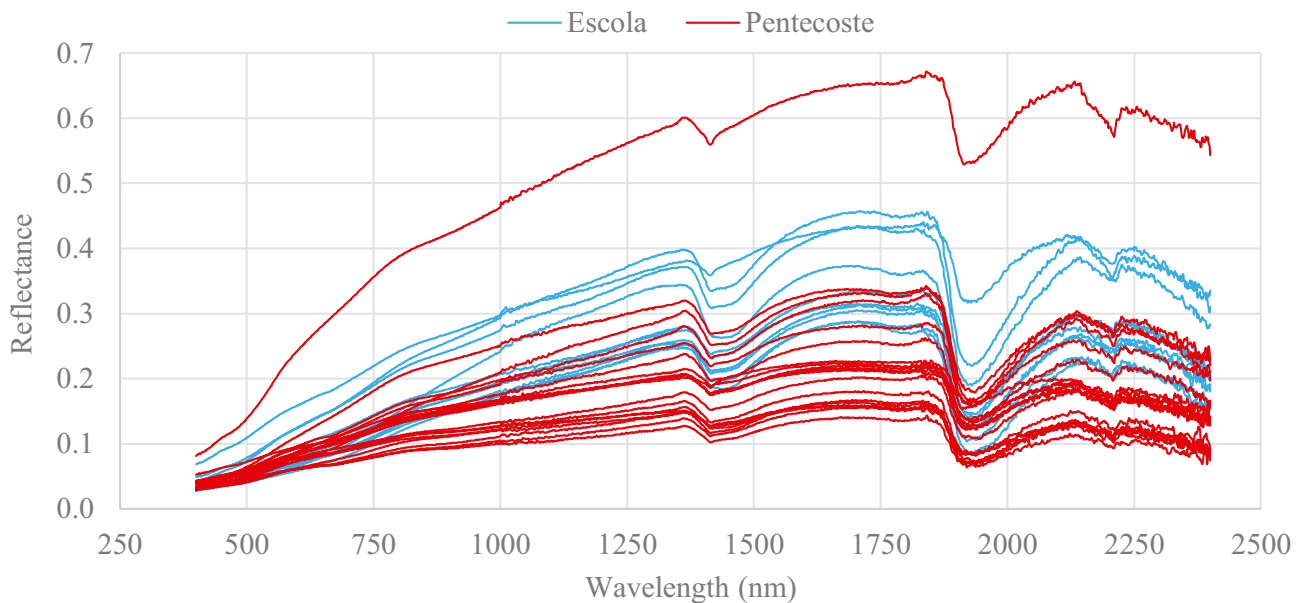


**Fig. 5** Spectra of the sediment samples in the Pentecoste catchment, before pre-processing

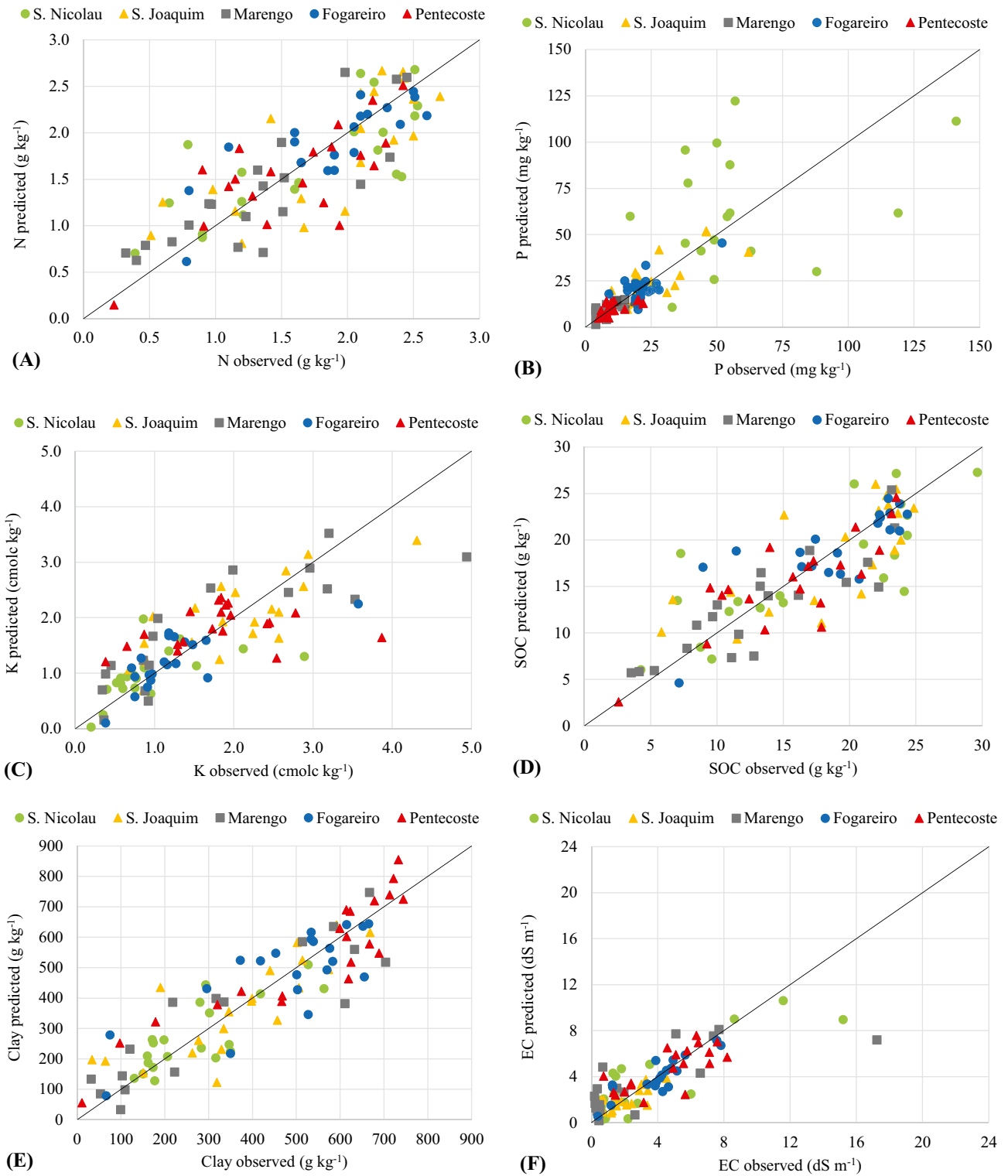


**Fig. 6** Results of cross-validation (leave-one-out) of models for individual reservoirs (<math>40 \text{ km}^2</math>): **A** nitrogen, **B** phosphorus, **C** potassium, **D** soil organic carbon, **E** clay, and **F** electrical conductivity

**Table 3** Calibrated models and their performance for characterization of sediments from spectroscopy at the reservoir-scale

Reservoir	Attribute	Calibrated models				Models' performance			
		NF <sup>b</sup>	Intercept	Slope	Bias	R <sup>2</sup>	RMSE	RPD	NSE
São Nicolau ( <i>n</i> <sup>a</sup> =20)	N	3	0.63	0.627	-0.001	0.58	0.46	1.57	0.58
	P	9	36.00	0.519	3.308	0.50	47.40	1.45	0.50
	K	2	0.50	0.443	0.015	0.30	0.55	1.17	0.23
	SOC	3	5.45	0.666	0.226	0.61	4.59	1.64	0.61
	Clay	6	81.30	0.704	-1.713	0.61	77.16	1.61	0.60
	EC	8	1.00	0.659	0.107	0.69	2.21	1.83	0.69
São Joaquim ( <i>n</i> <sup>a</sup> =20)	N	4	0.45	0.741	0.029	0.58	0.44	1.50	0.53
	P	4	8.53	0.679	-0.118	0.55	8.77	1.47	0.51
	K	10	0.79	0.608	-0.010	0.62	0.54	1.67	0.62
	SOC	4	5.42	0.698	0.178	0.54	4.08	1.45	0.50
	Clay	2	94.80	0.743	-0.187	0.66	99.30	1.73	0.65
	EC	10	0.69	0.634	-0.011	0.63	0.71	1.70	0.63
Marengo ( <i>n</i> <sup>a</sup> =20)	N	3	0.29	0.813	-0.042	0.69	0.37	1.75	0.66
	P	1	5.46	0.495	0.023	0.45	3.49	1.37	0.44
	K	5	0.38	0.722	0.071	0.63	0.81	1.64	0.61
	SOC	4	2.85	0.755	0.427	0.75	3.07	2.03	0.74
	Clay	4	26.10	0.901	0.972	0.85	96.90	2.59	0.84
	EC	8	1.14	0.529	0.156	0.49	2.98	1.43	0.48
Fogareiro ( <i>n</i> <sup>a</sup> =20)	N	7	0.66	0.662	-0.024	0.66	0.30	1.74	0.65
	P	5	8.57	0.612	-0.028	0.49	5.93	1.40	0.46
	K	9	0.54	0.548	0.005	0.54	0.42	1.52	0.54
	SOC	7	6.22	0.683	-0.197	0.60	3.12	1.61	0.59
	Clay	8	152.0	0.693	-6.482	0.62	104.27	1.64	0.61
	EC	6	1.06	0.730	0.024	0.75	0.93	2.06	0.75
Pentecoste ( <i>n</i> <sup>a</sup> =20)	N	8	0.49	0.670	0.036	0.52	0.40	1.42	0.47
	P	3	6.15	0.384	0.200	0.27	3.66	1.16	0.22
	K	1	1.60	0.128	-0.023	0.08	0.74	1.05	0.05
	SOC	8	3.77	0.744	0.250	0.64	3.25	1.67	0.62
	Clay	5	96.80	0.836	-10.475	0.83	89.19	2.47	0.83
	EC	4	1.24	0.714	0.026	0.59	1.59	1.56	0.57

<sup>a</sup>Number of sediment sampling points

<sup>b</sup>Number of factors in the PLSR models

The overall performance at the reservoir scale benefits from their relatively small areas, which tend to present more homogeneous factors controlling the sediment characteristics and transport conditions: soil type, land use, and hydrological regime. Similar findings have been reported by other authors investigating soil attributes with spectral data. For instance, Morellos et al. (2016) found good N and SOC estimations ( $R^2 > 0.70$ ) for small areas ( $\sim 0.30 \text{ km}^2$ ), and Franceschini et al. (2015) also found good model performance to estimate organic matter, K and clay in small areas ( $\sim 0.02 \text{ km}^2$ ) using PLSR.

At the catchment and regional scales, slight overestimation of lower values and underestimation of higher values are observed for SOC. In fact, Ward et al. (2019) reported a similar effect, and explained that it is caused by the skewness of the SOC distribution and changes in the relationship between

SOC and spectra for higher values. In our study, out of the 60 data samples (combination of six sediment properties in 10 reservoirs), 45% are highly skewed ( $|\text{skewness}| \geq 1$ ), 33% are moderately skewed ( $0.5 \leq |\text{skewness}| < 1$ ), and only 22% are approximately symmetric ( $|\text{skewness}| < 0.5$ ).

Whereas the models for estimating sediment attributes from spectral data seem reliable and potentially replicable in areas up to  $40 \text{ km}^2$  at the reservoir scale in the study region, application to larger extents on a regional basis is challenging. At the catchment scale (Benguê, Pentecoste, and Fogareiro catchments, with areas ranging from approximately  $1000$  to  $5000 \text{ km}^2$ ) and regional scale (which embraces two large basins: Jaguaribe, with  $74,000 \text{ km}^2$  and Curu, with  $8500 \text{ km}^2$ ), performance of the models degraded. This finding indicates that estimating sediment attributes from spectroscopy seems not to be feasible at very large spatial scales:

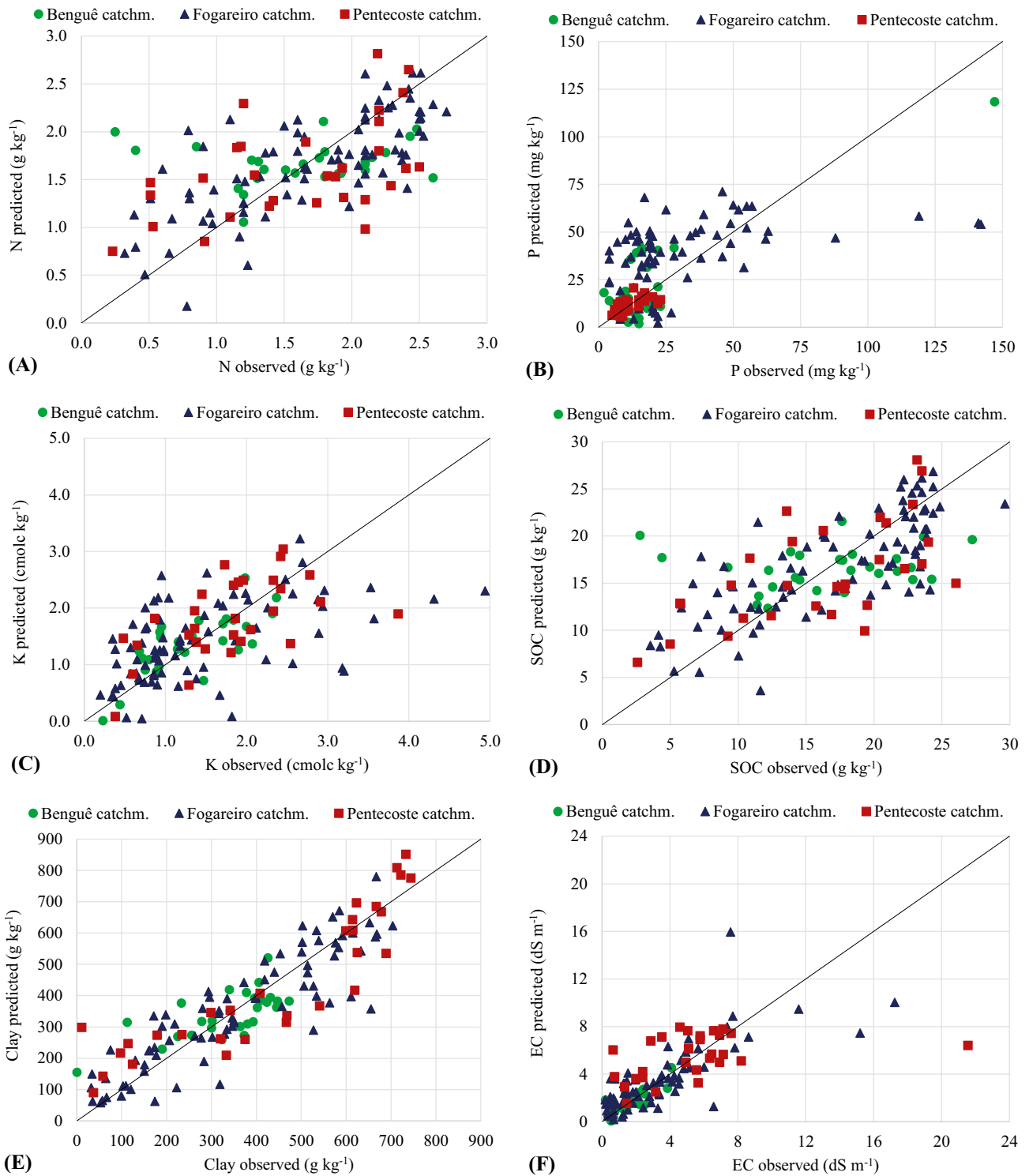


**Fig. 7** Results of cross-validation (leave-one-out) of models for catchments (900–6000 km<sup>2</sup>): **A** nitrogen, **B** phosphorus, **C** potassium, **D** soil organic carbon, **E** clay, and **F** electrical conductivity

**Table 4** Calibrated models and their performance for characterization of sediments from spectroscopy at the catchment-scale

Catchment	Attribute	Calibrated models				Models' performance			
		NF <sup>b</sup>	Intercept	Slope	Bias	R <sup>2</sup>	RMSE	RPD	NSE
Benguê catchment ( $n^a=28$ )	N	2	1.61	0.033	-0.019	0.01	0.59	0.98	-0.08
	P	12	3.95	0.794	-0.024	0.66	15.45	1.68	0.63
	K	10	0.44	0.692	-0.038	0.56	0.39	1.48	0.52
	SOC	2	15.70	0.053	-0.126	0.02	5.81	1.00	-0.04
	Clay	4	103.0	0.684	35.944	0.57	80.24	1.52	0.55
	EC	6	0.49	0.726	-0.014	0.60	0.60	1.56	0.57
Fogareiro catchment ( $n^a=80$ )	N	4	0.72	0.574	0.003	0.54	0.45	1.48	0.54
	P	2	29.10	0.163	0.348	0.12	41.71	1.06	0.10
	K	5	0.89	0.357	0.035	0.26	0.87	1.14	0.23
	SOC	5	6.29	0.629	0.009	0.58	4.24	1.53	0.57
	Clay	8	49.10	0.853	18.249	0.80	90.32	2.22	0.79
	EC	7	0.95	0.682	-0.002	0.59	2.07	1.54	0.57
Pentecoste catchment ( $n^a=30$ )	N	6	0.98	0.392	0.003	0.26	0.59	1.14	0.20
	P	3	6.10	0.477	-0.014	0.40	3.71	1.29	0.38
	K	6	0.93	0.499	-0.035	0.32	0.68	1.15	0.22
	SOC	7	7.93	0.506	-0.015	0.38	5.17	1.24	0.33
	Clay	4	82.20	0.823	-5.158	0.79	108.10	2.23	0.79
	EC	2	4.01	0.210	0.079	0.12	3.70	1.05	0.06

<sup>a</sup>Number of sediment sampling points

<sup>b</sup>Number of factors in the PLSR models

heterogeneity of sediment sources and processes contributing to sediment transport and deposition in reservoirs might not be captured by regression models.

Xu et al. (2018) reported that the performance of models to estimate soil or sediment attributes depends largely on the variability of the dataset. Due to differences in the source materials, sediments may have different physical and chemical characteristics, affecting the spectral response. In the future, methods to separate the dataset according to physico-chemical and/or spectral similarity rather than spatial origin, such as cluster analysis (Ward et al. 2019), may help improve model robustness.

Still, the indirect characterization of sediment from reservoirs' beds supports the practice of sediment reuse as fertilizer, by reducing the need for costly and time-consuming laboratory analyses. Thereby, the overall good performance of the models to predict clay content is crucial, as clay is a major physical characteristic controlling water flux and retention in the soil, impacting crop growth and productivity, especially in dry environments. Also, good model performance for EC at all the investigated scales is useful as a first assessment of the feasibility of sediment for reuse, by indicating reservoirs with high salinity that are unsuitable as nutrient sources for soil fertilization.

On the other hand, the low performance of most models for N, P, and K, especially at larger spatial scales, prevents accurate estimations of such fundamental nutrients for

crop production and, therefore, indicates a limitation of the approach adopted by us. Such results suggest that spectroscopy should not be the sole method to estimate nutrient content in sediments, but rather that it complements laboratory analyses. Improvements might be achieved with revision of the approach, e.g., by applying prior data transformations and/or clustering analyses as proposed by Ward et al. (2019), or adapting the (PLSR) model.

### 4.3 Influence of the spatial scale on sediment attribute estimation

Spatial scale is an important feature to consider when proposing regression models for sediment characterization, since higher heterogeneity of the factors controlling sediment composition (soil types, land use, sediment transport conditions) is expected as the spatial scale increases. Figure 9 presents the coefficients of determination ( $R^2$ ) of the regression models, according to the spatial scales as defined in Table 1.

From the graph, one can depict that an increase in the spatial scale of the reservoirs and from the aggregation of data of several reservoirs worsen the correlations, indicating that catchment and regional-scale models tend to be less accurate. This is particularly notable for P (to which the reduction of  $R^2$  is high, from roughly 0.5 to 0.25 at the reservoir and regional scales, respectively) and the other nutrients,

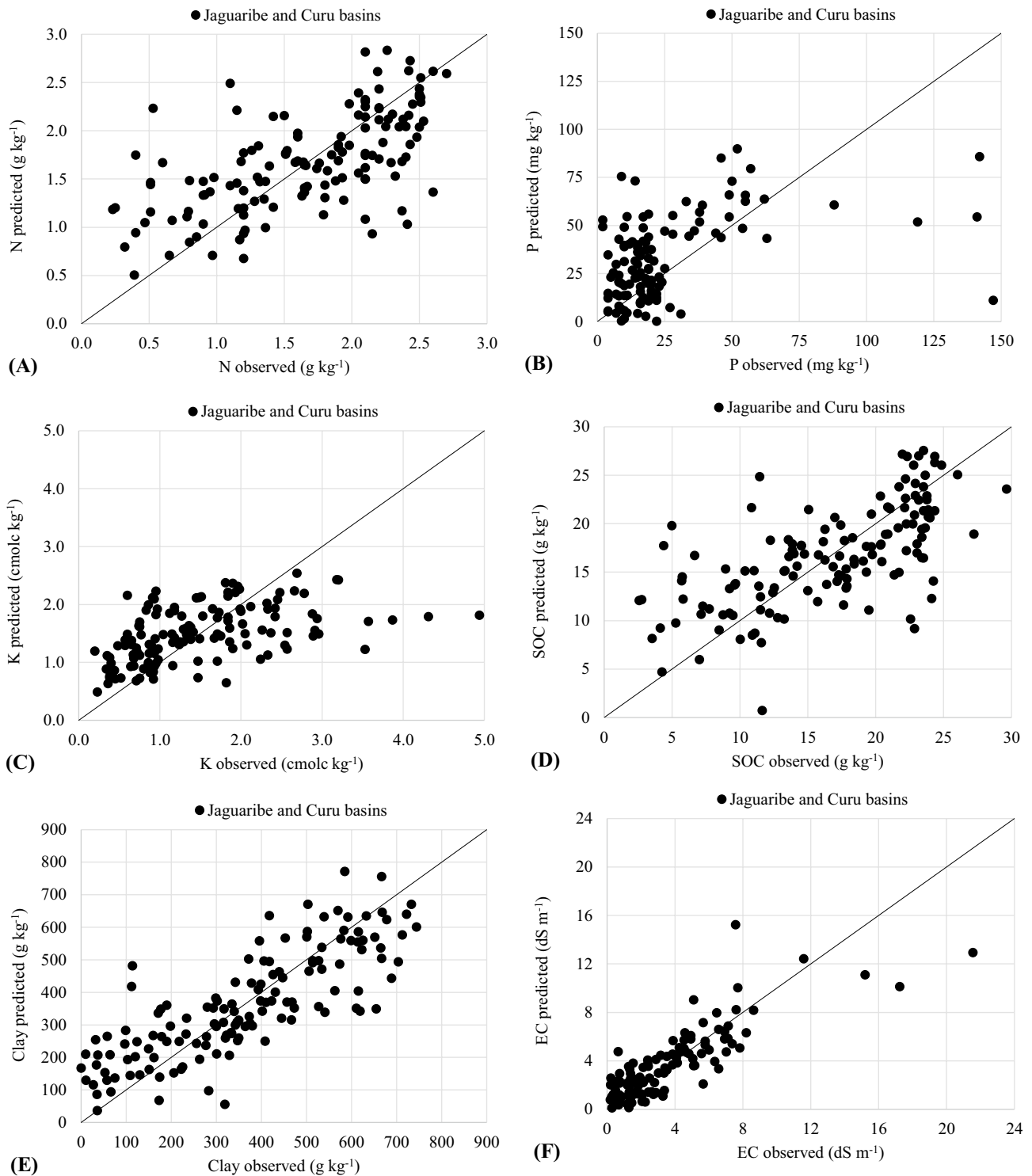


**Fig. 8** Results of cross-validation (leave-one-out) of models at the regional scale (82,500 km<sup>2</sup>): **A** nitrogen, **B** phosphorus, **C** potassium, **D** soil organic carbon, **E** clay, and **F** electrical conductivity

**Table 5** Calibrated models and their performance for characterization of sediments from spectroscopy at the regional-scale

Basin	Attribute	Calibrated models				Models' performance			
		NF <sup>b</sup>	Intercept	Slope	Bias	R <sup>2</sup>	RMSE	RPD	NSE
Jaguaribe and Curu basins ( $n^a = 138$ )	N	8	0.84	0.503	-0.010	0.38	0.52	1.23	0.34
	P	7	18.10	0.333	-0.229	0.24	33.10	1.12	0.20
	K	3	1.10	0.263	-0.002	0.24	0.77	1.15	0.24
	SOC	8	7.77	0.537	-0.063	0.42	4.91	1.29	0.39
	Clay	2	123.0	0.663	-0.996	0.65	117.62	1.70	0.65
	EC	10	0.82	0.735	0.026	0.69	1.80	1.81	0.69

<sup>a</sup>Number of sediment sampling points

<sup>b</sup>Number of factors in the PLSR models

whereas for clay and EC, the models tend to be more stable, with  $R^2$  around 0.7 in all scales.

From the abovementioned figure, three ranges of  $R^2$  can be identified according to the scale: for the reservoir scale (<40 km<sup>2</sup>),  $R^2$  tends to be higher and less variable (generally in the range of  $0.5 < R^2 < 0.8$ ); for the catchment scale (900–6000 km<sup>2</sup>), a decrease in  $R^2$  and higher variability can be observed ( $0.1 < R^2 < 0.7$ ); for the regional scale (82,500 km<sup>2</sup>), there is a strong tendency of degradation of the regression models' accuracy, with  $R^2$  usually below 0.4.

This result shows the role of spatial scale in estimating sediment attributes: sediment generated in larger areas tends to present higher heterogeneity (Silva et al. 2018), hampering its characterization from VNIR-SWIR spectroscopy and reducing the performance of prediction models. This finding suggests that homogeneous areas be established, for which the models could be transferred from one reservoir

to another without (re)calibration requiring physicochemical laboratory data. For instance, Ward et al. (2019) demonstrated that spectral clustering can improve soil organic carbon model performance compared to a reference model that was calibrated on the whole database without clustering. Furthermore, establishment of soil and sediment libraries, such as the Brazilian Soil Spectral Library — BSSL (Demattê et al. 2019b), has proven to potentially improve the capacity to predict the attributes at various spatial scales by identifying patterns of spectral signatures.

#### 4.4 Influence of the spectral resolution on sediment attribute estimation

By decreasing the spectral resolution down to 10 nm intervals, it was possible to assess its influence on the estimation of sediment attributes. Figure 10 presents the coefficients of

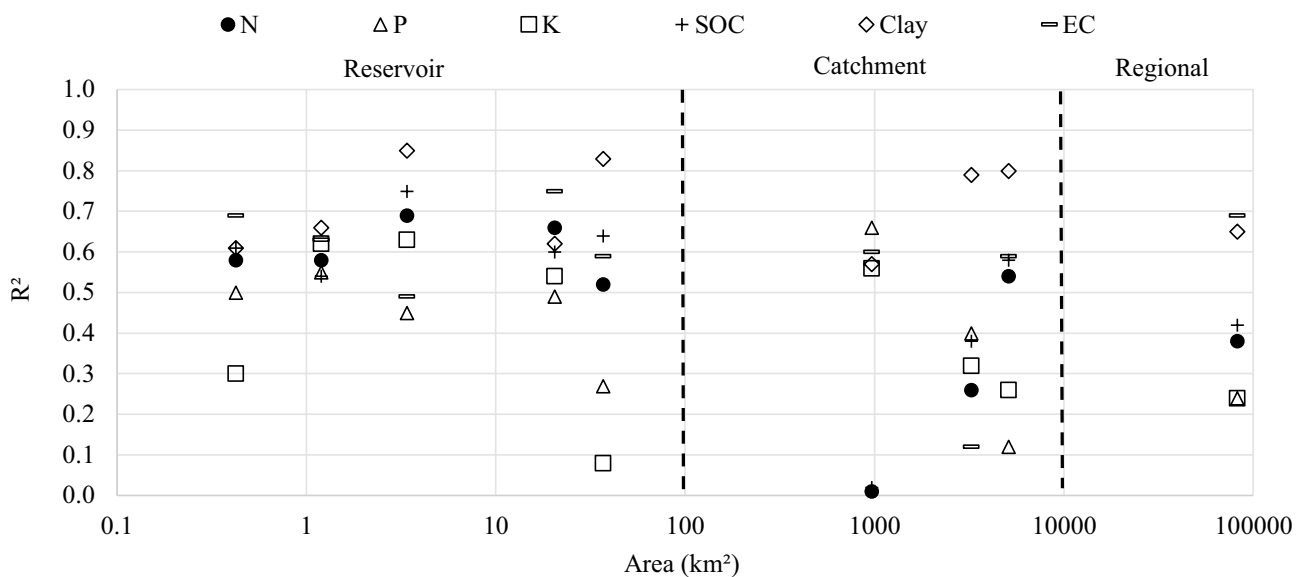


**Fig. 9** Influence of the spatial scale on the accuracy of regression models for estimating sediment attributes



determination ( $R^2$ ) of the models, at the reservoir (Fig. 10A) and catchment/regional scales (Fig. 10B).

Generally, very little impact is observed on the correlations between physicochemical and spectral characteristics when the spectral resolution is coarsened from 1 to 5 nm intervals: on average, the coefficient of determination is reduced by 1% at the reservoir scale, with only two models (out of 30 at this scale) with  $R^2$  decreasing more than 10%. At the catchment/

regional scale, the average reduction of  $R^2$  was 6%, and 4 models (out of 24) presented  $R^2$  reduction by more than 10%.

By decreasing the spectral resolution further down to 10 nm intervals, the correlations are maintained at the same level, with little influence of the spectral resolution on sediment attribute estimation. At the reservoir scale, average reduction of  $R^2$  (from 1 to 10 nm resolution coarsening) accounts for 2%, with over 10% reduction of  $R^2$  in 5 models.

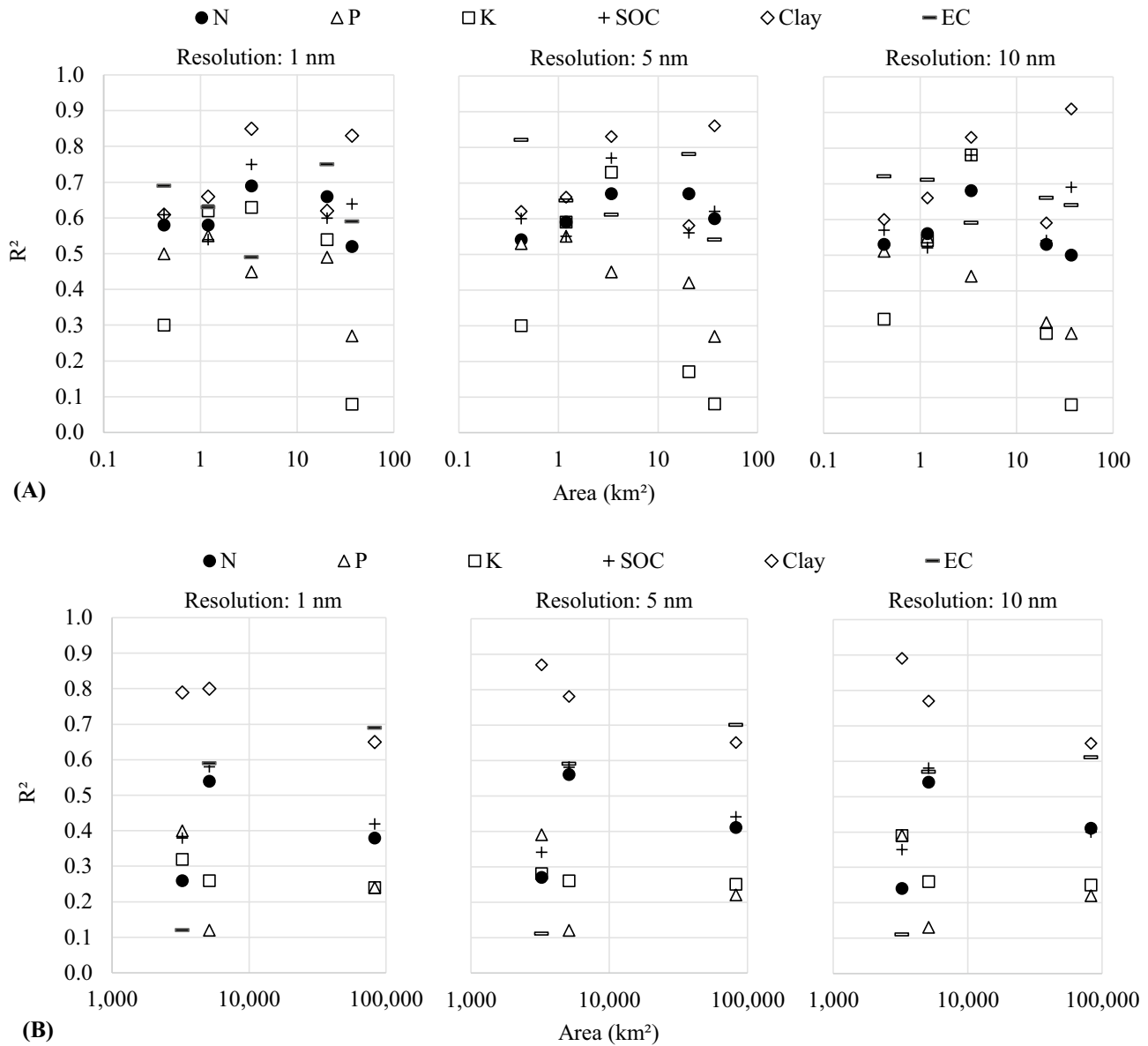


**Fig. 10** Influence of the spectral resolution on the accuracy of regression models for estimating sediment attributes at the reservoir **A** and catchment/regional **B** scales

At the catchment/regional scale, average reduction of  $R^2$  is 5%, and for 3 models,  $R^2$  reduction is higher than 10%. This is particularly important when analysing data that are originally captured at lower spectral resolutions, such as by hyperspectral satellite sensors, since coarsening of spectral resolution does not produce much degradation of the models' performance.

Similar results were found by Knadel et al. (2013), who tested the influence of different spectral resolutions up to 8 nm to estimate clay and SOC and found that lower spectral resolution did not affect model performance. Adeline et al. (2017) reported in their study that to estimate soil attributes, a reduction of spectral resolution caused a slight decrease in model prediction performance. Peng et al. (2014) performed spectral resampling between 2 and 10 nm on VNIR spectral data to estimate SOC, and found that, in general, there was little variation in the accuracy of the models. Yang et al. (2012) observed that calibration models for estimating soil N and C are insensitive to reduction of spectral resolution, and models with coarser resolution (e.g., 100 nm) presented very similar accuracy to those with 1 nm resolution.

Modelling based on spectroscopy, such as in this study, helps to build the knowledge necessary for the use of hyperspectral satellite imagery for soil and sediment characterization (Viscarra Rossel et al. 2006a). For instance, we demonstrate that model predictability is only slightly impacted by coarsening the spectral resolution up to 10 nm, which is in the range of the spectral sampling distance of the PRISMA hyperspectral satellite (lower than 11 nm in the VNIR and SWIR) (Cogliati et al. 2021) and the upcoming EnMAP hyperspectral satellite (6.5 nm in the VNIR and 10 nm in the SWIR) (Guanter et al. 2015). As argued by Braga et al. (2019), satellite-based remote sensing approaches may help not only to identify sediment properties, but also areas with nutrient deficiency in soils, enabling an optimization of the nutrient balance in catchments. However, the large pixel size of current and planned hyperspectral satellite missions, the limitation to the topsoil layer as well as soil and sediment cover, e.g., by litter can be challenging.

## 5 Conclusions and outlook

The use of VNIR-SWIR spectroscopy to estimate physicochemical sediment attributes in the semiarid region of Brazil has shown to be a promising approach for the characterization of sediments silted in surface water reservoirs.

Partial least square regression models performed in the range of good to very good in the prediction of clay and EC at spatial scales ranging from reservoirs (< 100 km<sup>2</sup>) up to regional (> 10,000 km<sup>2</sup>). The models for other sediment properties performed worse: for instance, SOC and N models were satisfactory to very good at the reservoir

scale, but degraded to unsatisfactory at the other spatial scales, whereas the models for P and K presented high variation, from unsatisfactory to satisfactory at all investigated scales. Such findings indicate that model performance is affected by heterogeneity of the factors controlling the sediment characteristics and transport conditions (soil type, land use, and hydrological regime), which tend to be higher in larger extents. Therefore, models tend to be more accurate when applied at small scales.

Coarsening of the spectral resolution in the range of 1 to 10 nm reduced the models' performance only slightly, not impacting the overall capacity of estimating the sediment attributes. This conclusion highlights the importance of field-based studies to estimate sediment attributes from VNIR-SWIR spectroscopy, as a step towards the application of hyperspectral satellite imagery to characterize the sediment from surface reservoirs' beds. Spectral resolution of satellites like PRISMA, EnMAP, and others are in the range tested by us in this study, but some hindrance still prevails, like the need for sediment exposure during the satellite passage, which implies empty reservoirs with no litter covering the bed. Despite the increasing availability of spaceborne imaging spectroscopy data, the methodology is not fully operational in terms of regular Earth observation yet and the temporal stability of sediment characteristics (in this region) needs to be assessed.

In general, spectroscopy-based indirect characterization of sediment supports the practice of sediment reuse as fertilizers, by reducing the costly and time-consuming laboratory analyses. The good performance on the estimation of clay is crucial, as it is a key feature controlling water flux and retention in the soil. Furthermore, reliable estimations of EC help to indicate the feasibility of sediment reuse, by identification of reservoirs with high salinity that are, therefore, unsuitable as nutrient source for soil fertilization.

However, lower performances for N, P, and K suggest that the proposed method needs improvement and be applied complementarily to laboratory analyses, as these are fundamental nutrients for soil fertilization.

**Supplementary Information** The online version contains supplementary material available at <https://doi.org/10.1007/s11368-022-03281-1>.

**Acknowledgements** We would like to thank Mai-Britt Berghöfer for her assistance in spectral data pre-processing and PLSR modelling.

**Funding** Open Access funding enabled and organized by the Project DEAL. The authors received PhD scholarship from the Brazilian Coordination for the Improvement of Higher Education Personnel (CAPES) granted to Thayslan Carvalho and funding for the research (PROBRAL, Grant 88881.371462/2019-01), financial support from the German Centre for Geosciences (GFZ) for the laboratory analyses, and support from the Brazilian National Council for Scientific and

Technological Development (CNPq) for Pedro Medeiros and Adunias Teixeira as research productivity fellows.

## Declarations

**Conflict of interest** The authors declare no competing interests.

**Open Access** This article is licensed under a Creative Commons Attribution 4.0 International License, which permits use, sharing, adaptation, distribution and reproduction in any medium or format, as long as you give appropriate credit to the original author(s) and the source, provide a link to the Creative Commons licence, and indicate if changes were made. The images or other third party material in this article are included in the article's Creative Commons licence, unless indicated otherwise in a credit line to the material. If material is not included in the article's Creative Commons licence and your intended use is not permitted by statutory regulation or exceeds the permitted use, you will need to obtain permission directly from the copyright holder. To view a copy of this licence, visit <http://creativecommons.org/licenses/by/4.0/>.

## References

- Adeline KRM, Gomez C, Gorretta N et al (2017) Predictive ability of soil properties to spectral degradation from laboratory Vis-NIR spectroscopy data. *Geoderma* 288:143–153. <https://doi.org/10.1016/j.geoderma.2016.11.010>
- Barnes RJ, Dhanoa MS, Lister SJ (1989) Standard normal variate transformation and de-trending of near-infrared diffuse reflectance spectra. *Appl Spectrosc* 43(5):772–777. <https://doi.org/10.1366/0003702894202201>
- Braga BB, Nunes Júnior FH, Barbosa RM et al (2017) Biomass production and antioxidative enzyme activities of sunflower plants growing in substrates containing sediment from a tropical reservoir. *J Agr Sci* 9:95–106. <https://doi.org/10.5539/jas.v9n5p95>
- Braga BB, Carvalho TRA, Brosinsky A et al (2019) From waste to resource: cost-benefit analysis of reservoir sediment reuse for soil fertilization in a semiarid catchment. *Sci Total Environ* 670:158–169. <https://doi.org/10.1016/j.scitotenv.2019.03.083>
- Brevik EC, Cerdà A, Mataix-Solera J et al (2015) The Interdisciplinary Nature of Soil Soil 1:117–129. <https://doi.org/10.5194/soil-1-117-2015>
- Brils J, de Boer P, Mulder J et al (2014) Reuse of dredged material as a way to tackle societal challenges. *J Soils Sediments* 14(9):1638–1641. <https://doi.org/10.1007/s11368-014-0918-0>
- Calixto Júnior JT, Drumond MA (2014) Estudo comparativo da estrutura fitossociológica de dois fragmentos de Caatinga em níveis diferentes de conservação. *Braz J for Res* 34:80. <https://doi.org/10.4336/2014.pfb.34.80.670>
- Capra GF, Grilli E, Macci C et al (2015) Lake-dredged material (LDM) in pedotechnique for the restoration of Mediterranean soils affected by erosion/entisolization processes. *J Soils Sediments* 15:32–46. <https://doi.org/10.1007/s11368-014-0950-0>
- Ceará (2009) Cadernos Regionais do Pacto das Águas. Conselho de Altos Estudos e Assuntos Estratégicos, Assembleia Legislativa do Estado do Ceará. Eudoro Walter de Santana (Coord.). Fortaleza: INESP
- Coeelho CF, Heim B, Foerster S et al (2017) In situ and satellite observation of CDOM and chlorophyll-a dynamics in small water surface reservoirs in the Brazilian Semiarid Region. *Water* 9:913. <https://doi.org/10.3390/w9120913>
- Cogliati S, Sarti F, Chiarantini L et al (2021) The PRISMA imaging spectroscopy mission: overview and first performance analysis. *Remote Sens Environ* 262:112499. <https://doi.org/10.1016/j.rse.2021.112499>
- Cozzolino D (2016) Near infrared spectroscopy as a tool to monitor contaminants in soil, sediments and water — state of the art, advantages and pitfalls. *Trends Environ Anal Chem* 9:1–7. <https://doi.org/10.1016/j.teac.2015.10.001>
- de Araújo JC, Guentner A, Bronstert A (2006) Loss of reservoir volume by sediment deposition and its impact on water availability in semiarid Brazil. *Hydrolog Sci J* 51(1):157–170. <https://doi.org/10.1623/hysj.51.1.157>
- de Araújo JC, Medeiros PHA (2013) Impact of dense reservoir networks on water resources in semiarid environments. *Australas J Water Resour* 17:87–100. <https://doi.org/10.7158/13241583.2013.11465422>
- de Figueiredo JV, de Araújo JC, Medeiros PHA et al (2016) Runoff initiation in a preserved semiarid Caatinga small watershed, Northeastern Brazil. *Hydrol Process* 30:2390–2400. <https://doi.org/10.1002/hyp.10801>
- Decock C, Lee J, Necpalova M et al (2015) Mitigating N<sub>2</sub>O emissions from soil: from patching leaks to transformative action. *Soil* 1:687–694. <https://doi.org/10.5194/soil-1-687-2015>
- Demattê JAM, Dotto AC, Bedin LG et al (2019a) Soil analytical quality control by traditional and spectroscopy techniques: constructing the future of a hybrid laboratory for low environmental impact. *Geoderma* 337:111–121. <https://doi.org/10.1016/j.geoderma.2018.09.010>
- Demattê JAM, Dotto AC, Paiva AFS et al (2019b) The Brazilian Soil Spectral Library (BSSL): a general view, application and challenges. *Geoderma* 354:113793. <https://doi.org/10.1016/j.geoderma.2019.05.043>
- EMBRAPA (2011) O novo mapa de solos do Brasil: legenda atualizada. Empresa Brasileira de Pesquisa Agropecuária - EMBRAPA, Ministério da Agricultura, Pecuária e Abastecimento. Rio de Janeiro - RJ, Brasil
- EMBRAPA (2017) Centro Nacional de Pesquisa dos Solos (Rio de Janeiro, RJ). Manual de métodos de análise de solo. Empresa Brasileira de Pesquisa Agropecuária - EMBRAPA, Rio de Janeiro - RJ, Brasil
- Fonseca R, Barriga FJAS, Fyfe WS (1998) Reversing desertification by using dam reservoir sediments as agriculture soils. *Episodes* 21:218–224. <https://doi.org/10.18814/epiugs/1998/v21i4/001>
- Franceschini MHD, Demattê JAM, da Silva TF et al (2015) Prediction of soil properties using imaging spectroscopy: considering fractional vegetation cover to improve accuracy. *Int J Applied Earth Obs Geoinf* 38:358–370. <https://doi.org/10.1016/j.jag.2015.01.019>
- Gomez C, Viscarra Rossel RA, McBratney AB (2008) Soil organic carbon prediction by hyperspectral remote sensing and field vis-NIR spectroscopy: an Australian case study. *Geoderma* 146(3–4):403–411. <https://doi.org/10.1016/j.geoderma.2008.06.011>
- Guanter L, Kaufmann H, Segl K et al (2015) The EnMAP Spaceborne Imaging Spectroscopy Mission for Earth Observation. *Remote Sens* 7(7):8830–8857. <https://doi.org/10.3390/rs70708830>
- Hu XY (2013) Application of visible/near-infrared spectra in modeling of soil total phosphorus. *Pedosphere* 23(4):417–421. [https://doi.org/10.1016/S1002-0160\(13\)60034-X](https://doi.org/10.1016/S1002-0160(13)60034-X)
- INMET (2018) Normas Climatológicas do Brasil 1981–2010. Instituto Nacional de Meteorologia - INMET, Ministério da Agricultura, Pecuária e Abastecimento. Brasília - DF, Brasil
- Junakov N, Balintov M (2012) Assessment of nutrient concentration in reservoir bottom sediments. *Procedia Eng* 42:165–170. <https://doi.org/10.1016/j.proeng.2012.07.407>
- Knadel M, Stenberg B, Deng F et al (2013) Comparing predictive abilities of three visible-near infrared spectrophotometers for soil organic carbon and clay determination. *J Near Infrared Spec* 21:67–80. <https://doi.org/10.1255/jnirs.1035>

- Kuang B, Mouazen AM (2011) Calibration of visible and near infrared spectroscopy for soil analysis at the field scale on three European farms. *Eur J Soil Sci* 62:629–636. <https://doi.org/10.1111/j.1365-2389.2011.01358.x>
- Lira CCS, Medeiros PHA, Lima Neto IE (2020) Modelling the impact of sediment management on the trophic state of a tropical reservoir with high water storage variations. *Ann Braz Acad Sci* 92(1):e20181169. <https://doi.org/10.1590/0001-3765202020181169>
- Lu P, Wang L, Niu Z et al (2013) Prediction of soil properties using laboratory VIS-NIR spectroscopy and Hyperion imagery. *J Geochem Explor* 132:26–33. <https://doi.org/10.1016/j.gexplo.2013.04.003>
- Ludwig B, Vormstein S, Niebuhr J et al (2017) Estimation accuracies of near infrared spectroscopy for general soil properties and enzyme activities for two forest sites along three transects. *Geoderma* 288:37–46. <https://doi.org/10.1016/j.geoderma.2016.10.022>
- Mamede GL, Guentner A, Medeiros PHA et al (2018) Modeling the effect of multiple reservoirs on water and sediment dynamics in a semiarid catchment in Brazil. *J Hydrol Eng* 23(12):05018020–05018021. [https://doi.org/10.1061/\(ASCE\)HE.1943-5584.0001701](https://doi.org/10.1061/(ASCE)HE.1943-5584.0001701)
- Mattei P, Pastorelli R, Rami G et al (2017) Evaluation of dredged sediment co-composted with green waste as plant growing media assessed by eco-toxicological tests, plant growth and microbial community structure. *J Hazard Mater* 333:144–153. <https://doi.org/10.1016/j.jhazmat.2017.03.026>
- Medeiros PHA, de Araújo JC, Mamede GL et al (2014) Connectivity of sediment transport in a semiarid environment: a synthesis for the Upper Jaguaribe Basin, Brazil. *J Soils Sediments* 14:1938–1948. <https://doi.org/10.1007/s11368-014-0988-z>
- Medeiros PHA, Sivapalan M (2020) From hard-path to soft-path solutions: slow-fast dynamics of human adaptation to droughts in a water scarce environment. *Hydrol Sci J* 65:1803–1814. <https://doi.org/10.1080/02626667.2020.1770258>
- Moreira LCJ, Teixeira AS, Galvão LS (2015) Potential of multispectral and hyperspectral data to detect saline-exposed soils in Brazil. *Giscience and Remote Sens* 52:1–21. <https://doi.org/10.1080/15481603.2015.1040227>
- Morellos A, Pantazi XE, Moshou D et al (2016) Machine learning based prediction of soil total nitrogen, organic carbon and moisture content by using VIS-NIR spectroscopy. *Biosyst Eng* 152:104–116. <https://doi.org/10.1016/j.biosystemseng.2016.04.018>
- Morgan CLS, Waiser TH, Brown DJ et al (2009) Simulated in situ characterization of soil organic and inorganic carbon with visible near-infrared diffuse reflectance spectroscopy. *Geoderma* 151:249–256. <https://doi.org/10.1016/j.geoderma.2009.04.010>
- Moriasi DN, Arnold JG, Van Liew MW et al (2007) Model evaluation guidelines for systematic quantification of accuracy in watershed simulations. *Trans Am Soc Agr Biol Eng* 50(3):885–900. <https://doi.org/10.13031/2013.23153>
- Moura DS, Lima Neto IE, Clemente A et al (2020) Modeling phosphorus exchange between bottom sediment and water in tropical semiarid reservoirs. *Chemosphere* 246:125686. <https://doi.org/10.1016/j.chemosphere.2019.125686>
- Nawar S, Mouazen AM (2017) Predictive performance of mobile vis-near infrared spectroscopy for key soil properties at different geographical scales by using spiking and data mining techniques. *CATENA* 151:118–129. <https://doi.org/10.1016/j.catena.2016.12.014>
- Ollobarren P, Capra A, Gelsomino A et al (2016) Effects of ephemeral gully erosion on soil degradation in a cultivated area in Sicily (Italy). *CATENA* 145:334–345. <https://doi.org/10.1016/j.catena.2016.06.031>
- Peng X, Shi T, Song A et al (2014) Estimating soil organic carbon using VIS/NIR spectroscopy with SVM and SPA methods. *Remote Sens* 6(4):2699–2717. <https://doi.org/10.3390/rs6042699>
- Santos JCN, Andrade EM, Guerreiro MJS et al (2016) Effect of dry spells and soil cracking on runoff generation in a semiarid micro watershed under land use change. *J Hydrol* 541:1057–1066. <https://doi.org/10.1016/j.jhydrol.2016.08.016>
- Savitzky A, Golay MJ (1964) Smoothing and differentiation of data by simplified least squares procedures. *Anal Chem* 36:1627–1639. <https://doi.org/10.1021/ac60214a047>
- Sigua GC, Holtkamp ML, Coleman SW (2004) Assessing the efficacy of lake-dredged materials from Lake Panasoffkee, Florida: implication to environment and agriculture. Part 1 – Soil and Environmental Quality Aspect. *Environ Sci Pollut R* 11:321–326. <https://doi.org/10.1007/BF02979646>
- Sigua GC (2009) Recycling biosolids and lake-dredged materials to pasture-based animal agriculture: alternative nutrient sources for forage productivity and sustainability. *A Review Agron Sustain Dev* 11(6):143–160. <https://doi.org/10.1051/agro:2008037>
- Silva EMR, Medeiros PHA, de Araújo JC (2018) Applicability of fingerprinting for identification of sediment sources in a mesoscale semiarid catchment. *J Braz Assoc Agr Eng* 38(4):553–562. <https://doi.org/10.1590/1809-4430-Eng.Agric.v38n4p553-562/2018>
- Silveira PR, Mamede GL (2021). Avaliação da aplicação de modelos de desprendimento em bacia experimental do semi-árido brasileiro. *Braz J Phys Geogr* 14:396–406. <https://doi.org/10.26848/rbfg.v14.1.p396-406>
- Tesfaye MA, Bravo-Oviedo A, Bravo F et al (2015) Selection of tree species and soil management for simultaneous fuelwood production and soil rehabilitation in the Ethiopian central highlands. *Land Degrad Dev* 26:665–679. <https://doi.org/10.1002/ldr.2268>
- Vägen TG, Shepherd KD, Walsh MG (2006) Sensing landscape level change in soil fertility following deforestation and conversion in the highlands of Madagascar using Vis-NIR spectroscopy. *Geoderma* 133:281–294. <https://doi.org/10.1016/j.geoderma.2005.07.014>
- Viscarrá Rossel RA, Walvoort DJJ, McBratney AB et al (2006a) Visible, near infrared, mid infrared or combined diffuse reflectance spectroscopy for simultaneous assessment of various soil properties. *Geoderma* 131(1–2):59–75. <https://doi.org/10.1016/j.geoderma.2005.03.007>
- Viscarrá Rossel RA, McGlynn RN, McBratney AB (2006b) Determining the composition of mineral-organic mixes using UV-vis-NIR diffuse reflectance spectroscopy. *Geoderma* 137(1–2):70–82. <https://doi.org/10.1016/j.geoderma.2006.07.004>
- Viscarrá Rossel RA (2008) ParLeS: Software for chemometric analysis of spectroscopic data. *Chemometr Intell Lab* 90(1):72–83. <https://doi.org/10.1016/j.chemolab.2007.06.006>
- Wang YB, Huang TY, Liu J et al (2015) Soil pH value, organic matter and macronutrients contents prediction using optical diffuse reflectance spectroscopy. *Comput Electron Agr* 111:69–77. <https://doi.org/10.1016/j.compag.2014.11.019>
- Ward KJ, Chabrilat S, Neumann C et al (2019) A remote sensing adapted approach for soil organic carbon prediction based on the spectrally clustered LUCAS soil database. *Geoderma* 353:297–307. <https://doi.org/10.1016/j.geoderma.2019.07.010>
- Wohl E, Barros A, Brunsell N et al (2012) The hydrology of the humid tropics. *Nat Clim Change* 2:655–662. <https://doi.org/10.1038/nclimate1556>
- Wold S, Sjöström M, Eriksson L (2001) PLS-regression: a basic tool of chemometrics. *Chemometr Intell Lab* 58(2):109–130. [https://doi.org/10.1016/S0169-7439\(01\)00155-1](https://doi.org/10.1016/S0169-7439(01)00155-1)
- Xu S, Zhao Y, Wang M et al (2018) Comparison of multivariate methods for estimating selected soil properties from intact soil cores of paddy fields by Vis-NIR spectroscopy. *Geoderma* 310:29–43. <https://doi.org/10.1016/j.geoderma.2017.09.013>
- Yang H, Kuang B, Mouazen AM (2012) Quantitative analysis of soil nitrogen and carbon at a farm scale using visible and near infrared spectroscopy coupled with wavelength reduction. *Eur J*

Soil Sci 63:410–420. <https://doi.org/10.1111/j.1365-2389.2012.01443.x>

Zhang S, Foerster S, Medeiros P et al (2016) Bathymetric survey of water reservoirs in north-eastern Brazil based on TanDEM-X satellite data. *Sci Total Environ* 571:575–593. <https://doi.org/10.1016/j.scitotenv.2016.07.024>

Zhang S, Waske B, de Araújo JC et al (2018) Effective water surface mapping in macrophyte-covered reservoirs in NE Brazil based on

TerraSAR-X time series. *Int J Applied Earth Obs Geoinf* 69:41–55. <https://doi.org/10.1016/j.jag.2018.02.014>

**Publisher's Note** Springer Nature remains neutral with regard to jurisdictional claims in published maps and institutional affiliations.